



ELSEVIER

Performance Evaluation 49 (2002) 341–358

**PERFORMANCE
EVALUATION**
An International
Journal

www.elsevier.com/locate/peva

Second-order stochastic fluid models with fluid-dependent flow rates

Dongyan Chen^{a,*}, Yiguang Hong^{a,b}, Kishor S. Trivedi^a

^a *Department of Electrical and Computer Engineering, Center for Advanced Computing and Communications (CACC), Duke University, Durham, NC 27708-0294, USA*

^b *Institute of Systems Science, Chinese Academy of Sciences, Beijing 100080, China*

Abstract

In this paper, the analysis of second-order stochastic fluid models, where the fluid rate is dependent on the fluid level, is addressed. The boundary conditions are presented for the fluid models under consideration, which have extended previous work with only reflecting barrier assumptions. To obtain the transient solution of the fluid dynamics, a finite difference solution method is presented, which confirms to the boundary conditions and satisfies the normalization condition at the same time. With our approach, the modeling power of second-order fluid models is directly extended to include the case with fluid-dependent rates. As an application example, a statistical multiplexing problem is analyzed with our proposed method.

© 2002 Elsevier Science B.V. All rights reserved.

Keywords: Second-order fluid models; Boundary conditions; Transient analysis; Finite difference method

1. Introduction

Stochastic fluid models, as an important category of the analytic models, have drawn considerable attention in such applications as the performance analysis of communication systems (see [1,2] and references therein). The strength of fluid modeling paradigm over discrete modeling methods lies in the fact that the fluid modeling complexity is not as sensitive to the transmission speed and the buffer size as of its discrete counterpart. This property has made fluid methods particularly attractive in modeling high speed communication system with large buffers, like ATM networks, where the discrete modeling methods may meet the so-called “state-space explosion” problem. Furthermore, fluid models can be conveniently applied to study the hybrid systems consisting of both discrete part and continuous part.

In general, two classes of fluid flow models are used, i.e., first-order models (described by first moments alone) and second-order models (also involving Brownian motion). In [1], the first-order fluid flow models were applied in the analysis of the ATM multiplexing problem with on-off fixed rate sources, and the steady-state solution was provided. Following that, the transient solution was treated by Ren and

* Corresponding author.

E-mail addresses: dc@ee.duke.edu (D. Chen), hong@ee.duke.edu (Y. Hong), kst@ee.duke.edu (K.S. Trivedi).

Kobayashi in [3] with Laplace transform method. Sericola [4] proposed a non-transform-based approach, known as *randomization* (or *uniformization*). Wolter [5] studied the transient analysis of fluid models with reflecting boundaries by finite difference method.

When the fluctuation in the fluid flow rate cannot be neglected as it exhibits certain “noisy” nature, first-order models employed to approximate the fluid flow may fail to achieve the desired modeling accuracy, as observed by Ang and Barria in [6]. In such cases, second-order fluid flow models come to play an important role as a more fine-grained modeling technique. In second-order models, the queue length/buffer content process is represented as a diffusion process (or Brownian motion) with drift and variance modulated by a finite state Markov chain. Karandikar and Kulkarni [7] have presented the system of partial differential equations (PDEs) describing the model dynamics. They addressed the infinite buffer case with fluid-independent flow rates, and used reflecting condition to describe the diffusion process behavior at lower and upper boundaries. They also gave a matrix decomposition/factorization method to obtain the steady-state solution.

The aforementioned research efforts on second-order flow models only consider the fluid-independent flow rate case, i.e., the flow rate associated with a certain discrete state does not change with the occupied buffer level. In the models where fluid rates are independent of fluid levels, boundaries are formed when fluid buffer is empty and when fluid level approaches either buffer limit (in finite buffer case) or infinity (in infinite buffer case). In these cases, the reflecting barrier may be an appropriate assumption. However, boundary conditions can become more complicated if fluid rates depend on the fluid levels. As will be seen in the following sections, additional boundaries may be formed between the upper and lower limits where reflecting barrier assumption is not appropriate to describe the fluid behavior at these boundaries. This class of fluid models is important in modeling buffer management problems in communication system design, where congestion control schemes are employed to adjust the data rate according to the buffer levels.

To fill this gap between fluid modeling theory and applications, we study the solution of second-order fluid models with fluid-dependent flow rates in this paper. According to the underlying fluid behavior at the boundaries, the environmental states (discrete states of the modulating CTMC) are classified as *fluid reflecting states*, *fluid absorbing states*, *fluid emitting states*, and *fluid isolating states*. For each class of states, a PDE is derived from the general governing equations to describe the fluid behavior at the boundary. By putting together the PDEs for all four classes of fluid states at the boundary with the governing equations, a system of coupled PDEs is derived for the model.

Next, we present a finite difference method to solve the system of coupled PDEs. One major obstacle in this approach is the conservation of probability mass, i.e., the probability mass of the whole system need to be 1 in each iteration from time t to $t + \Delta t$. In [5], the normalization condition is explicitly incorporated into the system of PDEs, requiring a system of linear equations to be solved. In our approach, we incorporate the normalization condition implicitly in the construction of the finite difference approximation around the boundary, so that the probability mass is conserved in each iteration. In this way, we do not need to solve the system of linear equations as in [5] and thus simplify the computations.

By solving the PDEs, transient measures of the system may be obtained. This technique may be used in the transient analysis of communication systems. As a numerical example, we show the application of the technique in the transient study of ATM statistical multiplexing problem, for such measures as system overshoot [8] and recovery time [9] under system overload or failures.

This paper is organized as follows. In Section 2, the concepts and governing equations of second-order fluid models with fluid-dependent flow rates are presented. Section 3 is devoted to the discussion of

the boundary conditions for both intermediate boundaries, formed by thresholds given in the middle of the buffer under consideration, and upper/lower boundaries. For every boundary condition, a system of PDEs is derived to depict the dynamic behavior of the Markov modulated diffusion process. Following that, a solution method of the system of coupled PDEs based on finite difference method is presented in Section 4. The application of second-order fluid models in the transient analysis of the statistical multiplexing problem in ATM networks is demonstrated in Section 5, with numerical results exhibited. Finally, Section 6 concludes the paper.

2. Fluid model and basic results

2.1. Basics

In this paper, a Markov modulated stochastic fluid process, denoted by $F(t) = (X(t), M(t))$ on state-space $[0, \infty) \times E$, is considered. The fluid level $X(t)$ is assumed to be a non-negative continuous random variable whose variation rate depends on the discrete state modulating process $M(t)$, which is a continuous-time Markov chain (CTMC) with a finite state-space $E = \{0, \dots, K\}$ (the number of states in E is $K + 1$). This formulation has been commonly used to study different Markovian models such as Markov modulated rate process (MMRP) and Markov modulated regulated Brownian motion (MMRBM) (for example, [1,7,6]). Let the infinitesimal generator matrix Q of the $\{M(t)\}$ process be

$$Q = \begin{bmatrix} q_{00} & q_{01} & \cdots & q_{0K} \\ q_{10} & q_{11} & \cdots & q_{1K} \\ \vdots & \vdots & \ddots & \vdots \\ q_{K0} & q_{K1} & \cdots & q_{KK} \end{bmatrix}, \tag{1}$$

where q_{ij} denotes the transition rate from state i to state j for states $i, j \in E, i \neq j$, with $q_{ii} = -\sum_{j \neq i} q_{ij}$.

We consider the second-order stochastic fluid model. As per the Brownian motion theory [10], the increment $X(t+h) - X(t)$ in the $\{X(t), t \geq 0\}$ process over $[t, t+h]$ under a given environmental state k is assumed to be normally distributed with mean r_k and variance σ_k^2 . In other words, while $M(t)$ stays in state k , the $X(t)$ process is a Brownian motion with drift r_k and variance $\sigma_k^2, k \in E$. To this end, we define the drift and variance parameters as

$$\lim_{h \rightarrow 0} \frac{E[X(t+h) - X(t) | M(t) = k]}{h} \Big|_{X(t)=x} = r_k(x), \tag{2}$$

$$\lim_{h \rightarrow 0} \frac{\text{Var}[X(t+h) - X(t) | M(t) = k]}{h} \Big|_{X(t)=x} = \sigma_k^2(x). \tag{3}$$

Define the cumulative distribution function (CDF) of the fluid process $(X(t), M(t))$ as

$$P(t, x, k) = \Pr\{X(t) \leq x \text{ and } M(t) = k\}, \tag{4}$$

and let $\mathbf{P}(t, x) = [P(t, x, k), k \in E]$ be a row vector of CDFs of all discrete states $k \in E$.

Similarly, at points where the CDF $P(t, x, k)$ is differentiable, the probability density function (pdf) is defined as

$$p(t, x, k) = \lim_{\Delta x \rightarrow 0} \frac{\Pr\{x < X(t) \leq x + \Delta x, M(t) = k\}}{\Delta x} = \frac{\partial P(t, x, k)}{\partial x},$$

and $\mathbf{p}(t, x) = [p(t, x, k), k \in E]$ is a row vector of pdf's for all the discrete states.

It is worthwhile to point out that probability mass may be accumulated at certain point b under discrete environmental state m , and will result in discontinuities in CDF $P(t, b, k)$, which can be expressed as $P(t, b^-, k) \neq P(t, b^+, k)$. At these points, $(\partial/\partial x)P(t, x, k)$ does not exist. To this end, we use the probability mass function (pmf) to show this difference, which is denoted by

$$c(t, b, k) = \Pr\{X(t) = b, M(t) = k\} = P(t, b^+, k) - P(t, b^-, k).$$

Let

$$g(t, x, k) = p(t, x, k) + \sum_{c(t, \zeta, k) > 0} c(t, \zeta, k) \delta(x - \zeta), \tag{5}$$

where $\delta(\cdot)$ is the Dirac delta function. Then, integration of $g(t, x, m)$ produces

$$P(t, x, k) = \int_{-\infty}^x g(t, x, k) = \int_{-\infty}^x p(t, x, k) dx + \sum_{\substack{\zeta \leq x \\ c(t, \zeta, k) > 0}} c(t, \zeta, k).$$

2.2. Governing equation

The behavior of the second-order fluid flow model is described by the corresponding Kolmogorov forward differential equation (or the Fokker–Planck equation) as stated in the following proposition, which can be derived in a way proposed in many references like [7].

Proposition 1. *For each state $i \in E$, the function $g(t, x, i)$ is governed by*

$$\frac{\partial g(t, x, i)}{\partial t} + \frac{\partial(g(t, x, i)r_i(x))}{\partial x} = \frac{1}{2} \frac{\partial^2(g(t, x, i)\sigma_i^2(x))}{\partial x^2} + \sum_{j \in E} g(t, x, j)q_{ji}(x). \tag{6}$$

In vector form, (6) can be written as

$$\frac{\partial \mathbf{g}(t, x)}{\partial t} + \frac{\partial(\mathbf{g}(t, x)R(x))}{\partial x} = \frac{\partial^2(\mathbf{g}(t, x)S(x))}{\partial x^2} + \mathbf{g}(t, x)Q(x), \tag{7}$$

where $\mathbf{g}(t, x) = [g(t, x, i), i \in E]$, $R(x) = \text{diag}[r_i(x), i \in E]$ is the mean flow rate matrix, and $S(x) = \text{diag}[\sigma_i^2(x)/2, i \in E]$ is the flow rate variance matrix. The quantity $\mathbf{f}(t, x) = \mathbf{g}(t, x)R(x) - \partial \mathbf{g}(t, x)S(x)/\partial x$ is called the probability density flux, since this measure represents the amount of probability density “flowing” through level x per unit time. The boundary conditions for the PDE (7) will be addressed in later sections.

Although the governing equations are given by Proposition 1, they are not amenable to direct numerical solution due to the delta functions in $\mathbf{g}(t, x)$. For this reason, we treat the pmf's separately from the pdf's. By integrating both sides of (6), we obtain the following theorem.

Theorem 1. The pmf $\mathbf{c}(t, x)$ is governed by

$$\begin{aligned} \frac{\partial c(t, x, i)}{\partial t} + \frac{\partial c(t, x, i)r_i(x)}{\partial x} + p(t, x^+, i)r_i(x^+) - \frac{1}{2} \frac{\partial (p(t, x^+, i)\sigma_i^2(x^+))}{\partial x} - p(t, x^-, i)r_i(x^-) \\ + \frac{1}{2} \frac{\partial (p(t, x^-, i)\sigma_i^2(x^-))}{\partial x} = \sum_{j \in E} c(t, b, j)q_{ji}(b) \quad \forall i \in E, \end{aligned} \tag{8}$$

where $x^+ = \lim_{\Delta x \rightarrow 0}(x + \Delta x)$, and $x^- = \lim_{\Delta x \rightarrow 0}(x - \Delta x)$.

Equivalently, we have

$$\begin{aligned} \frac{\partial \mathbf{c}(t, x)}{\partial t} + \frac{\partial \mathbf{c}R}{\partial x} \mathbf{p}(t, x^+)R(x^+) - \frac{\partial (\mathbf{p}(t, x^+)S(x^+))}{\partial x} - \mathbf{p}(t, x^-)R(x^-) \\ + \frac{\partial (\mathbf{p}(t, x^-)S(x^-))}{\partial x} = \mathbf{c}(t, x)Q(x), \end{aligned} \tag{9}$$

where $\mathbf{c}(t, x) = [c(t, x, i), i \in E]$ and $\mathbf{p}(t, x) = [p(t, x, i), i \in E]$.

If $\mathbf{c}(t, x) = 0$, the pdf $\mathbf{p}(t, x)$ is given by

$$\frac{\partial \mathbf{p}(t, x)}{\partial t} + \frac{\partial (\mathbf{p}(t, x)R(x))}{\partial x} = \frac{\partial^2 (\mathbf{p}(t, x)S(x))}{\partial x^2} + \mathbf{p}(t, x)Q(x). \tag{10}$$

Proof. First note that the probability mass can only exist at discrete points. To determine the equation for $\mathbf{c}(x)$, integrate (6) from x^- to x^+ , i.e.,

$$\begin{aligned} \int_{x^-}^{x^+} \frac{\partial \mathbf{g}(t, x)}{\partial t} dx + \int_{x^-}^{x^+} \frac{\partial}{\partial x} (\mathbf{g}(t, x)R(x)) dx \\ = \int_{x^-}^{x^+} \frac{\partial^2 (\mathbf{g}(t, x)S(x))}{\partial x^2} dx + \int_{x^-}^{x^+} \mathbf{g}(t, x)Q(x) dx. \end{aligned} \tag{11}$$

Substitute all the $\mathbf{g}(t, x)$ with $\mathbf{h}(t, x)$ and $\mathbf{c}(t, x)$ by (5), the equation becomes (9).

If $\mathbf{c}(t, x) = 0$, $\mathbf{g}(t, x) = \mathbf{p}(t, x)$. After substituting $\mathbf{g}(t, x)$ with $\mathbf{p}(t, x)$ in (7), we get Eq. (10). \square

By letting $c(t, x, i) = 0, i \in E$ in (8), we have the following corollary.

Corollary 1. When no probability mass is accumulated at fluid level x , the probability density flux at this point is continuous, which is

$$p(t, b^+, k)r_k(b^+) - \frac{1}{2} \frac{\partial (p(t, b^+, k)\sigma_k^2(b^+))}{\partial x} = p(t, b^-, k)r_k(b^-) - \frac{1}{2} \frac{\partial (p(t, b^-, k)\sigma_k^2(b^-))}{\partial x}, \tag{12}$$

where

$$\frac{\partial}{\partial x} (p(t, b^+, k)\sigma_k^2(b^+)) = \left. \frac{\partial}{\partial x} (p(t, x, k)\sigma_k^2(x)) \right|_{x \downarrow b},$$

and

$$\frac{\partial}{\partial x} (p(t, b^-, k)\sigma_k^2(b^-)) = \left. \frac{\partial}{\partial x} (p(t, x, k)\sigma_k^2(x)) \right|_{x \uparrow b}.$$

Corollary 1 is of critical importance in the treatment of those points where the fluid flow of some discrete states changes in magnitude but not in direction. In such a case, no probability mass is accumulated, and the property of continuity in probability density flux is applied to obtain the probability density after the change.

As mentioned before, to study practical problems, the boundary conditions have to be taken into consideration for the solution to the governing PDEs in [Theorem 1](#).

3. Boundary conditions

In this section, the problem of boundary conditions is discussed. When the buffer capacity is constrained, its lower and upper boundaries are formed naturally by the fact that the fluid inside the buffer cannot exceed these levels. Meanwhile, boundaries can also form in the middle of the buffer level, where the flow rates change their values or directions abruptly. In this paper, r_k and σ_k are regarded as the functions of the fluid level, denoted by x . For simplicity of presentation, we only consider the case where the flow rate is assumed to be a piecewise constant function of x . The set of boundary points, Z , is then defined as

$$Z = \{x | \exists k \in E, r_k(x^+) \neq r_k(x^-), X_0 \leq x \leq X_m\},$$

where X_0 and X_m are the lower and upper boundaries, respectively. This means that the boundaries are formed at those points where the fluid flow of any of the environmental states changes rate.

Second-order fluid flows with only lower and upper boundaries have been investigated, where reflecting behavior is assumed for all the environmental states [5–7]. Other than reflecting boundaries, sticky or absorbing boundaries [10–12] are also used to better approximate realistic applications. Nevertheless, reflecting boundary assumption is most commonly used due to its simplicity.

For the problem under investigation in this paper, i.e., when intermediate boundaries exist, the reflecting behavior is then no longer an appropriate assumption. As an illustrative example, consider an environmental state k where the fluid rate associated with this environmental state, $(r_k(x), \sigma_k(x))$, only changes value but does not change direction across the intermediate boundary. Under reflection boundary assumption, the probability that the fluid process associated with this environmental state flowing across the boundary is zero, since it is “reflected” on the boundary. However, this is not true in reality. To this end, more complex type of boundaries need to be adopted to better reflect the physical behavior of the system.

As will be discussed later, intermediate boundaries may exhibit very different properties to different environmental states, according to the fluid rate associate with them. For this reason, we classify the environmental states according to their mean flow rates around the boundary. A graphical illustration of this classification is shown in [Fig. 1](#). The mean flow rate around the boundary of a given environmental state may exhibit the four different patterns represented by S1–S4. We assume $x = X_0$ and X_m are the lower and upper boundaries, respectively, and $x = b$ is an intermediate boundary. The downward arrow is used to represent a negative mean flow rate at the corresponding fluid level, and the upward arrow is used to represent a positive mean flow rate at the corresponding fluid level. As an example, the mean flow rate for environmental states belonging to pattern S1 is negative when the fluid level $b < x < X_m$, and is positive when the fluid level $X_0 < x < b$. Note that the upper boundary is a special case of boundary $x = b$ where for each discrete state $k \in E$, $r_k(b^+) = 0$ and $r_k(b^-) \neq 0$ with $\sigma_k(b^+) = 0$. Similarly,

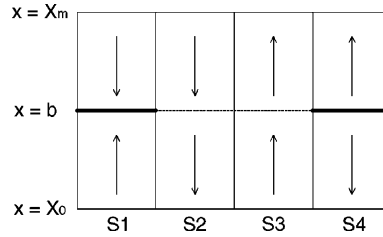


Fig. 1. The fluid behavior around the boundary.

the lower boundary is a special case of boundary b where for each discrete state $k \in E$, $r_k(b^-) = 0$ and $r_k(b^+) \neq 0$ with $\sigma_k(b^-) = 0$.

In the following sections, we will show that the boundary $x = b$ may exhibit *absorbing* or *isolating* behavior for environmental states with flow rates satisfying conditions S1 and S4, and may exhibit *emitting* behavior for environmental states with flow rates satisfying conditions S2 and S3. For this reason, at each boundary, the environmental states, rather than the boundary itself, are classified. Specifically, at each boundary we classify the environmental states as fluid absorbing states, fluid emitting states, fluid reflecting states, and fluid isolating states. The word *fluid* is added to distinguish these states from the terminologies in Markov chain theory.

Based on r_k and σ_k , we define the following partition of E :

$$\begin{aligned}
 E_{1+}(x) &= \{k \in E : \sigma_k^2(x) > 0, r_k(x) > 0\}, & E_{10}(x) &= \{k \in E : \sigma_k^2(x) > 0, r_k(x) = 0\}, \\
 E_{1-}(x) &= \{k \in E : \sigma_k^2(x) > 0, r_k(x) < 0\}, & E_{0+}(x) &= \{k \in E : \sigma_k^2(x) = 0, r_k(x) > 0\}, \\
 E_{00}(x) &= \{k \in E : \sigma_k^2(x) = 0, r_k(x) = 0\}, & E_{0-}(x) &= \{k \in E : \sigma_k^2(x) = 0, r_k(x) < 0\}. \quad (13)
 \end{aligned}$$

Denote

$$E_1(x) = E_{1+}(x) \cup E_{10}(x) \cup E_{1-}(x), \quad E_0(x) = E_{0+}(x) \cup E_{00}(x) \cup E_{0-}(x), \quad (14)$$

where $E_1(x)$ is the set of all discrete states with non-zero variance in flow rates, and $E_0(x)$ the set of all discrete states with zero variance in flow rates.

We also have observed that fluid behavior at upper/lower boundary is different from that at the boundary in between. For clarity of representation, these boundaries are treated separately. For this purpose, we define both the upper and lower boundaries as *terminal boundaries*, and the boundaries formed inside the buffer as *intermediate boundaries*.

3.1. Intermediate boundaries

Consider the boundary points $b \in Z$ with $X_0 < b < X_m$ as well as $r_k(b^-)$ and $r_k(b^+)$ non-zero for all $k \in E$, where the conventional Brownian motion model is no longer applicable to describe the diffusion process behavior near the boundary because of the abrupt change of flow rates across the boundary.

To simplify the solution of this problem when intermediate boundaries exist, the environmental states are classified into the following three boundary states according to the fluid behavior near the boundary: fluid absorbing states, fluid isolating states, and fluid emitting states.

3.1.1. Absorbing states

Consider condition S1 in Fig. 1, which indicates that the mean flow rate of a discrete state is positive (incoming flow) when the buffer level is less than b , and is negative (outgoing flow) when the buffer level is larger than b .¹ In this situation, the fluid level is pushed from both upper and lower sides of the boundary.

Assume the flow rate at the boundary of absorbing states is

$$r_k(b) = 0 \quad \text{and} \quad \sigma_k^2(b) = 0 \quad \text{if} \quad k : r_k(b^-) > 0 \quad \text{and} \quad r_k(b^+) < 0,$$

which means that the fluid has to stay at the boundary once it has reached there. With this assumption, the probability mass is accumulated on the boundary, and *absorbing* property is exhibited, because the fluid is pushed from both sides of the boundary.

Therefore, the set of absorbing states is defined as

$$K_a(b) = \{k | r_k(b^-) > 0 \quad \text{and} \quad r_k(b^+) < 0\}.$$

Note that the following analysis is limited only for the second-order case for simplicity of presentation, that is, $k \in E_{1-}(b^+) \cap E_{1+}(b^-)$.²

The probability mass accumulated on the boundary is represented as

$$c(t, b, k) = \Pr\{X(t) = b, M(t) = k\} > 0 \quad \forall k \in K_a(b).$$

With the assumption that the boundary location does not change with fluid level in the buffer, from (8) we have

$$\begin{aligned} \frac{\partial c(t, b, k)}{\partial t} = & \underbrace{\sum_{i \in E} c(t, b, i) q_{ik}(b)}_1 - \underbrace{p(t, b^+, k) r_k(b^+) + \frac{1}{2} \frac{\partial (p(t, b^+, k) \sigma_k^2(b^+))}{\partial x}}_2 \\ & + \underbrace{p(t, b^-, k) r_k(b^-) - \frac{1}{2} \frac{\partial (p(t, b^-, k) \sigma_k^2(b^-))}{\partial x}}_3, \\ p(t, b^-, k) = p(t, b^+, k) = & 0 \quad \forall k \in K_a(b). \end{aligned} \tag{15}$$

An intuitive explanation of (15) is that the contribution to the changes in the probability mass constitutes two parts: one is the transfer of probability mass among different states (item 1 on the r.h.s. of (15)), and the other is the probability mass flowing into (item 2 on the r.h.s. of (15)) or out of this boundary (item 3 on the r.h.s. of (15)).

3.1.2. Emitting states

For the discrete state k whose mean fluid rate r_k does not change direction and satisfies condition S2 or S3, there is no probability mass accumulated at the boundary, and the probability mass transferred from other states are converted to changes in probability densities.

¹ Such a control mechanism is employed to avoid congestion in the ATM multiplexing problem, where the incoming fluid flow is restricted when the cells in the buffer exceed a certain threshold [1].

² The discussion of absorbing states in the first-order case is given in [13].

The set of emitting states is defined as

$$K_e(b) = \{k | r_k(b^-)r_k(b^+) > 0\}.$$

Since the fluid level cannot stay at the boundary, no probability mass can accumulate at these points (referring to [11]).

Again, applying (8) gives

$$\begin{aligned} p(t, b^+, k)r_k(b^+) - \frac{1}{2} \frac{\partial(p(t, b^+, k)\sigma_k^2(b^+))}{\partial x} - p(t, b^-, k)r_k(b^-) + \frac{1}{2} \frac{\partial(p(t, b^-, k)\sigma_k^2(b^-))}{\partial x} \\ = \sum_{i \notin K_e} c(t, b, i)q_{ik}(b), \quad c(t, b, k) = 0 \quad \forall k \in K_e(b), \end{aligned} \tag{16}$$

which shows that the variation in the probability density flux of the emitting states at boundary b equals the probability mass transferred from other states.

3.1.3. Isolating states

The discrete state whose rate around the boundary b satisfies condition S4 is called an *isolating state*, since the queue levels become divergent in this state at $x = b$.

Then the set of isolating states can be given as

$$K_i(b) = \{k | r_k(b^-) < 0 \text{ and } r_k(b^+) > 0\}.$$

In this state, the probability mass transferred from other states cannot be converted to probability density flux, and it just stays at the boundary. Since there is no contribution from the probability density flux to the variation of the probability mass, the boundary condition is derived from (8) as

$$\begin{aligned} \frac{dc(t, x, k)}{dt} = \sum_{i \in E} c(t, b, i)q_{ik}(b) + \frac{1}{2} \frac{\partial(p(t, b^+, k)\sigma_k^2(b^+))}{\partial x} - \frac{1}{2} \frac{\partial(p(t, b^-, k)\sigma_k^2(b^-))}{\partial x}, \\ p(t, b^+, k) = p(t, b^-, k) = 0 \quad \forall k \in K_i(b). \end{aligned} \tag{17}$$

3.2. Terminal boundaries

At terminal boundaries, discrete states where flow rates have non-zero variance (that is, $\sigma_k \neq 0$ for given k) can be viewed as *reflecting states* as was done in many references, while the discrete states with zero variance in the associated flow rates can be classified into *absorbing states* and *emitting states*. The discussion of the last two cases where the fluid model becomes first-order due to zero variance may also be found in the references such as [13].

3.2.1. Reflecting states

This class of states has been well treated in the literature. An equivalent description of the behavior of diffusion process at the upper and lower boundaries can be obtained from a diffusion process without boundary through the imposition of a lower control barrier at the lower boundary and an upper control barrier at the upper boundary [10]. These control barriers are called *regulators*. It is proved in [10] that when the fluid model can be represented as regulated by the boundary regulators, no probability mass can accumulate at the boundaries, and its boundaries have the reflection property. This justifies the reflecting

boundary argument in previous research in this field, such as in [7]. Similar results are obtained by Ang and Barria [6], who analyzed a second-order fluid flow process having a finite capacity buffer with the help of two-sided regulators. For this reason, we specify reflecting boundary at the upper and the lower boundaries for all the discrete states with non-zero variance in flow rate.

The set of reflecting states at boundary b is defined as

$$K_r(b) = \{k | k \in E_1(b), b = X_0 \text{ or } b = X_m\}.$$

Since the probability mass cannot accumulate at the boundary of reflecting states, we have the following.

Following (8), the boundary condition can be written as

$$\begin{aligned} p(t, b^+, k)r_k(b^+) - \frac{1}{2} \frac{\partial(p(t, b^+, k)\sigma_k^2(b^+))}{\partial x} - p(t, b^-, k)r_k(b^-) + \frac{1}{2} \frac{\partial(p(t, b^-, k)\sigma_k^2(b^-))}{\partial x} \\ = \sum_{i \notin K_r} c(t, b, i)q_{ik}(b), \quad c(t, b, k) = 0 \quad \forall k \in K_r(b) \end{aligned} \quad (18)$$

with the fact that $p(t, X_0^-, i) = 0$ and $p(t, X_m^+, i) = 0$ by definition.

An intuitive explanation of (18) is that the probability density flux at the boundary of the reflecting states can only be varied by the injection (transfer) from (to) the probability mass in other states.

3.2.2. Absorbing states

The set of absorbing states is defined as

$$K_a(b) = \{k | k \in E_{0+}(b^-), b = X_m\} \cup \{k | k \in E_{0-}(b^+), b = X_0\}.$$

For the absorbing states at the terminal boundaries, the fluid flow presents first-order behavior. When the boundary is reached, the fluid stays at that level. Therefore, probability mass is accumulated and $c(t, b, k) > 0 \forall k \in K_a(b)$.

The governing equation can thus be derived from (15) by letting $\sigma_k^2(b^+) = \sigma_k^2(b^-) = 0 \forall k \in K_a(b)$:

$$\frac{\partial c(t, b, k)}{\partial t} = \sum_{i \in E} c(t, b, i)q_{ik}(b) - p(t, b^+, k)r_k(b^+) + p(t, b^-, k)r_k(b^-) \quad \forall k \in K_a(b). \quad (19)$$

3.2.3. Emitting states

The set of emitting states is defined as

$$K_e(b) = \{k | k \in E_{0+}(b^-), b = X_m\} \cap \{k | k \in E_{0-}(b^+), b = X_0\}.$$

Again, for the emitting states at the terminal boundaries, the fluid flow presents first-order behavior and no probability mass can accumulate (i.e., $c(t, b, k) = 0$ for all $k \in K_r(b)$). From (8), we have

$$p(t, b^+, k)r_k(b^+) - p(t, b^-, k)r_k(b^-) = \sum_{i \in E} c(t, b, i)q_{ik}(b) \quad \forall k \in K_a(b). \quad (20)$$

4. Solution using the finite difference method

In this section, we present algorithms based on the finite difference method to solve the system of coupled PDEs for the transient analysis of the model. By letting time t approach infinity, steady-state

results may also be obtained. We have extended the work in [5] by considering the more complex boundary conditions mentioned in the last section. Moreover, the numerical analysis is simpler because the normalization condition is incorporated in the construction of finite difference equations, rather than being treated as an additional constraint.

For simplicity, we only consider the ‘pure second-order’ case in this paper where $\sigma_k \neq 0$ for all $k = 0, \dots, K$. The construction of finite difference method for a model where both first-order and second-order flows are present can be directly derived from the discussion of the second-order case based on the ideas similar to those proposed here.

4.1. Finite difference approximation

The discretization of (10) is carried out on an equidistant grid with step size Δt in time direction and step size Δx in space direction. In this way, the pdf $p(t, x, k)$ is approximated by the discrete function at the grid point as

$$u_{k,j}^n \approx p(n\Delta t, j\Delta x, k),$$

and the rate function is discretized as

$$r_{k,j} \approx r_k(j\Delta x), \quad \sigma_{k,j}^2 \approx \sigma_k^2(j\Delta x).$$

The time derivative is discretized with a forward difference quotient

$$\frac{\partial}{\partial t} p(n\Delta t, j\Delta x, k) \approx \frac{u_{k,j}^{n+1} - u_{k,j}^n}{\Delta t},$$

and the first-order space derivative is discretized as follows:

$$\frac{\partial}{\partial x} (p(n\Delta t, j\Delta x, k)r_{k,j}) \approx \begin{cases} \frac{u_{k,j}^n r_{k,j} - u_{k,j-1}^n r_{k,j-1}}{\Delta x}, & r_{k,j} > 0, \\ \frac{u_{k,j+1}^n r_{k,j+1} - u_{k,j}^n r_{k,j}}{\Delta x}, & r_{k,j} < 0. \end{cases}$$

The second derivative is discretized with a central difference

$$\frac{\partial^2}{\partial x^2} (p(n\Delta t, j\Delta x, k)\sigma_k^2(j\Delta x)) \approx \frac{u_{k,j+1}^n \sigma_{k,j+1}^2 - 2u_{k,j}^n \sigma_{k,j}^2 + u_{k,j-1}^n \sigma_{k,j-1}^2}{\Delta x^2}.$$

Then the discrete approximation of (10) is

$$\begin{aligned} & \frac{u_{k,j}^{n+1} - u_{k,j}^n}{\Delta t} + \frac{u_{k,j}^n r_{k,j} - u_{k,j-1}^n r_{k,j-1}}{\Delta x} - \frac{1}{2} \frac{u_{k,j+1}^n \sigma_{k,j+1}^2 - 2u_{k,j}^n \sigma_{k,j}^2 + u_{k,j-1}^n \sigma_{k,j-1}^2}{\Delta x^2} \\ & = \sum_{m \in E} u_{m,3}^n q_{mk}, \quad r_{k,j} > 0, \\ & \frac{u_{k,j}^{n+1} - u_{k,j}^n}{\Delta t} + \frac{u_{k,j+1}^n r_{k,j+1} - u_{k,j}^n r_{k,j}}{\Delta x} - \frac{1}{2} \frac{u_{k,j+1}^n \sigma_{k,j+1}^2 - 2u_{k,j}^n \sigma_{k,j}^2 + u_{k,j-1}^n \sigma_{k,j-1}^2}{\Delta x^2} \\ & = \sum_{m \in E} u_{m,3}^n q_{mk}, \quad r_{k,j} < 0. \end{aligned} \tag{21}$$

4.2. Treatment of boundary conditions

In this section, we consider discretization at boundaries. As may be noted, the group of PDEs and ordinary differential equations (ODEs) presented in the last section are not sufficient to obtain the numerical transient results by finite difference approach. An important but unapplied condition for the solution of the fluid model is the constraint that the integration of the probability density in all the states equals 1. In this paper, we apply this condition in the finite difference method by *conservation of probability mass*, which is to guarantee that the probability mass will not be *lost* in iterations by the construction of the finite difference format at the boundaries. In subsequent discussions, the finite difference method for various states at the boundary is addressed.

Given $b \in Z$, we use $B = (b - X_0) \bmod \Delta x + 1$ to represent the segment just below the boundary b , and $B + 1$ is therefore the segment just above the boundary b . The pdf $p(t, b^+, k)$ and $p(t, b^-, k)$ around the boundary is then approximated by the discrete function

$$u_{k,B+1}^n \approx p(n\Delta t, b^+, k),$$

and

$$u_{k,B}^n \approx p(n\Delta t, b^-, k).$$

In the following, we will address the discretization of each boundary discussed in the previous sections.

4.2.1. Reflecting states

The location of the boundary for the reflecting states is either at $b = X_0$ or X_m . First consider the boundary $b = X_0$ (and thus $B = 1$) and reflecting state k with $k \in E_r(X_0)$ and $r_k(X_0^+) > 0$ (i.e., $k \in E_r(X_0) \cap E_{1+}(X_0^+)$). The discretization of the PDE around $u_{k,1}^n$ is then

$$\frac{u_{k,1}^{n+1} - u_{k,1}^n}{\Delta t} + \frac{\overbrace{u_{k,1}^n r_{k,1}}^1 - \overbrace{u_{k,0^+}^n r_{k,0^+}}^2}{\Delta x} - \frac{1}{2} \frac{\overbrace{u_{k,2}^n \sigma_{k,2}^2}^3 - \overbrace{2u_{k,1}^n \sigma_{k,1}^2}^4 + \overbrace{u_{k,0^+}^n \sigma_{k,0^+}^2}^5}{\Delta x^2} = \overbrace{\sum_{m \in E} u_{m,1}^n q_{mk}}^6. \tag{22}$$

Similarly, the discretizations of the PDE around $u_{k,2}^n$ and $u_{k,3}^n$ are

$$\frac{u_{k,2}^{n+1} - u_{k,2}^n}{\Delta t} + \frac{\overbrace{u_{k,2}^n r_{k,2}}^1 - \overbrace{u_{k,1}^n r_{k,1}}^2}{\Delta x} - \frac{1}{2} \frac{\overbrace{u_{k,3}^n \sigma_{k,3}^2}^3 - \overbrace{2u_{k,2}^n \sigma_{k,2}^2}^4 + \overbrace{u_{k,1}^n \sigma_{k,1}^2}^5}{\Delta x^2} = \sum_{m \in E} u_{m,2}^n q_{mk}, \tag{23}$$

$$\frac{u_{k,3}^{n+1} - u_{k,3}^n}{\Delta t} + \frac{\overbrace{u_{k,3}^n r_{k,3}}^1 - \overbrace{u_{k,2}^n r_{k,2}}^2}{\Delta x} - \frac{1}{2} \frac{\overbrace{u_{k,4}^n \sigma_{k,4}^2}^3 - \overbrace{2u_{k,3}^n \sigma_{k,3}^2}^4 + \overbrace{u_{k,2}^n \sigma_{k,2}^2}^5}{\Delta x^2} = \sum_{m \in E} u_{m,3}^n q_{mk}. \tag{24}$$

To conserve the probability mass, the changes in $u_{k,1}$ from time t to $t + \Delta t$ need to be balanced by the construction of discretization format around the boundary. Items 1–6 in (22) represents the variations in probability density $u_{k,1}^n$ from time $n\Delta t$ to $(n + 1)\Delta t$. Among them, item 1 is cancelled out in (23), item 3 is cancelled out in (23) and (24), and item 4 is partially cancelled out in (23). Item 6 is the probability density

transfer from one discrete state to another discrete state, and will not introduce unbalanced probability mass. However, when there is probability mass accumulated at boundary $b = X_0$ in other discrete states, it may be transferred to state k . To conserve the probability mass from time $n\Delta t$ to $(n + 1)\Delta t$, the total unbalanced probability mass variation in $u_{k,1}^n \Delta x$ should be set equal to the probability mass transferred from the other discrete states, which produces

$$u_{k,0^+}^n r_{k,0^+} - \frac{1}{2} \frac{u_{k,1}^n \sigma_{k,1}^2 - u_{k,0^+}^n \sigma_{k,0^+}^2}{\Delta x} = \sum_{m \in E} c_{m,0}^n q_{mk}, \quad k \in K_r(0) \cap E_{1+}(0^+), \quad (25)$$

where $c_{m,0}^n \approx c(n\Delta t, b = X_0, m)$. Note that this equation is in fact the discrete approximation of (18).

This idea to keep probability masses balanced, which will be also used in the following, is actually equivalent to the normalization condition, that is, the total probability should be 1. Here this condition is not added as an additional constraint on finite difference approximation equations. Instead, the normalization condition is satisfied in given initial conditions at first, and then at each iterative step, with the above idea, the sum of all probability masses is kept unchanged. In this way, the normalization condition naturally holds, which leads to simple algorithms. By similar reasoning, the boundary treatment for other reflecting states is

$$u_{k,1}^n r_{k,1} - \frac{1}{2} \frac{u_{k,1}^n \sigma_{k,1}^2 - u_{k,0^+}^n \sigma_{k,0^+}^2}{\Delta x} = \sum_{m \in E} c_{m,0}^n q_{mk}, \quad k \in K_r(0) \cap E_{1-}(0^+), \quad (26)$$

$$-u_{k,I}^n r_{k,I} + \frac{1}{2} \frac{u_{k,X_m}^n \sigma_{k,X_m}^2 - u_{k,I}^n \sigma_{k,I}^2}{\Delta x} = \sum_{m \in E} c_{m,X_m}^n q_{mk}, \quad k \in K_r(X_m) \cap E_{1+}(X_m^-), \quad (27)$$

$$-u_{k,X_m}^n r_{k,X_m} + \frac{1}{2} \frac{u_{k,X_m}^n \sigma_{k,X_m}^2 - u_{k,I}^n \sigma_{k,I}^2}{\Delta x} = \sum_{m \in E} c_{m,X_m}^n q_{mk}, \quad k \in K_r(X_m) \cap E_{1-}(X_m^-). \quad (28)$$

4.2.2. Absorbing states

Performing the similar procedure, we have

$$\frac{c_{k,b}^{n+1} - c_{k,b}^n}{\Delta t} + u_{k,B+1}^n r_{k,B+1} - \frac{1}{2} \frac{u_{k,B+1}^n \sigma_{k,B+1}^2}{\Delta x} - \left(u_{k,B}^n r_{k,B} + \frac{1}{2} \frac{u_{k,B}^n \sigma_{k,B}^2}{\Delta x} \right) = \sum_{m \in E} c_{m,b}^n q_{mk}, \quad (29)$$

which can be viewed as the finite difference version of condition (15). As discussed in the analysis of reflecting states, the finite difference equations for the absorbing states naturally satisfy the normalization condition.

4.2.3. Emitting states

For emitting states, we have

$$u_{k,b^+}^n r_{k,b^+} - \frac{1}{2} \frac{u_{k,B+1}^n \sigma_{k,B+1}^2 - u_{k,b^+}^n \sigma_{k,b^+}^2}{\Delta x} - \left(u_{k,B}^n r_{k,B} - \frac{1}{2} \frac{u_{k,b^-}^n \sigma_{k,b^-}^2 - u_{k,B}^n \sigma_{k,B}^2}{\Delta x} \right) = \sum_{m \in E} c_{m,b}^n q_{mk}. \quad (30)$$

The value of u_{k,b^-} is not known beforehand and needs to be calculated. However, the finite difference approximation of the general PDE (10) cannot be applied here, since the second-order derivative of $p(t, b^-, k)$ does not exist. By assuming $\sigma^2 = 0$ at boundary b , we approximate the second-order behavior at b^- with first-order equations, which is

$$\frac{u_{k,b^-}^{n+1} - u_{k,b^-}^n}{\Delta t} + \frac{u_{k,b^-}^n r_{k,b^-} - u_{k,B}^n r_{k,B}}{\Delta x} = \sum_{m \in E} u_{m,b^-}^n q_{mk}.$$

In a similar manner, the treatment of states $k \in K_e(b) \cap E_{1-}(b^-) \cap E_{1-}(b^+)$ at the boundary is

$$\begin{aligned} & u_{k,B+1}^n r_{k,B+1} - \frac{1}{2} \frac{u_{k,B+1}^n \sigma_{k,B+1}^2 - u_{k,b^+}^n \sigma_{k,b^+}^2}{\Delta x} - \left(u_{k,b^-}^n r_{k,b^-} - \frac{1}{2} \frac{u_{k,b^-}^n \sigma_{k,b^-}^2 - u_{k,B}^n \sigma_{k,B}^2}{\Delta x} \right) \\ &= \sum_{m \in E} c_{m,b}^n q_{mk} \end{aligned}$$

and

$$\frac{u_{k,B+1}^{n+1} - u_{k,b^+}^n}{\Delta t} + \frac{u_{k,B+1}^n r_{k,B+1} - u_{k,b^+}^n r_{k,b^+}}{\Delta x} = \sum_{m \in E} u_{m,b^+}^n q_{mk}. \tag{31}$$

This is consistent with condition (16) and the normalization condition.

4.2.4. Isolating states

The finite difference computation for isolating states is

$$\frac{c_{k,b}^{n+1} - c_{k,b}^n}{\Delta t} - \frac{1}{2} \frac{u_{k,B+1}^n \sigma_{k,B+1}^2}{\Delta x} - \frac{1}{2} \frac{u_{k,B}^n \sigma_{k,B}^2}{\Delta x} = \sum_{m \in E} c_{m,b}^n q_{mk}. \tag{32}$$

It is easy to see that the preceding discussion is consistent with condition (17) and the normalization condition.

Assume the initial condition at $t = 0$ is $\mathbf{p}(0, x) = \mathbf{p}_0(x)$, $\mathbf{c}(0, x) = \mathbf{c}_0(x)$, the overall finite difference based algorithm to solve a second-order fluid model is as follows:

- (1) [Advance time step] $t = t + \Delta t$.
- (2) [Initialize] $\mathbf{p}(t, X_0^-) = \mathbf{p}(t, X_m^+) = 0$.
- (3) [Probability densities away from the boundary] Use (21) to obtain $\mathbf{p}(t + \Delta t, x)$, where $x \notin Z$.
- (4) [Probability densities at the boundary] For each boundary $X_0 < b < X_m$:
 - [Probability densities of non-absorbing states around the boundary] For all non-absorbing states k at boundary $x = b$, obtain $p(t, b^-, k)$ and $p(t, b^+, k)$ with corresponding boundary equations.
 - [Probability densities of absorbing states around the boundary] For all absorbing states k at boundary b , obtain $p(t, b^+, k)$ and $p(t, b^-, k)$ using (21).
 - [Probability mass accumulated on the boundary] For all absorbing states k at boundary $x = b$, obtain $\mathbf{c}(t, b)$ using (15) for intermediate boundaries, and using (19) for terminal boundaries.
- (5) [Termination] If $t > T_{\max}$, stop; else go to step 1.

5. A numerical example

In this section, an illustrative example of statistical multiplexing problem is given, which may be relevant with ATM multiplexer design. In our model, K statistically independent and identical on–off sources multiplexed by a common buffer with capacity X_m are considered. The duration of the on and off periods of each traffic source is exponentially distributed with mean $1/\alpha_1$ and $1/\alpha_0$, respectively. Whenever the source is in *on* state, it generates *priority cells* with rate λ_0 and *marked cells* with rate λ_1 .

When the buffer occupancy is less than a threshold b ($0 < b < X_m$), all incoming cells are accepted, and when the buffer occupancy is larger than b and less than X_m , the marked cells are dropped while the priority cells are accepted. When the buffer occupancy is 0 (meaning that the buffer is empty), the output flow rate is 0, and when the buffer occupancy is X_m (meaning that the buffer is full), all cells are dropped and the input flow rate is 0.

Since these K sources are statistically identical and independent, they could be aggregated and be represented by a CTMC with $K + 1$ discrete states $k = 0, 1, \dots, K$, where k is the number of sources that are in the *on* state. The infinitesimal generator matrix Q of this CTMC is given by

$$q_{ij} = \begin{cases} i\alpha_1, & j = i - 1, \\ (K - i)\alpha_0, & j = i + 1, \\ -i\alpha_1 - (K - i)\alpha_0, & j = i. \end{cases}$$

In state k , the net flow rate into the buffer can be expressed as follows:

$$r_k(x) = \begin{cases} k(\lambda_0 + \lambda_1) - c, & 0 < x < b, \\ k\lambda_0 - c, & b < x < X_m, \\ 0, & x = b, \\ \max(k(\lambda_0 + \lambda_1) - c, 0), & x = 0, \\ \min(k\lambda_0 - c, 0), & x = X_m, \end{cases} \tag{33}$$

where x is the fluid level of the buffer.

Take two independent traffic sources, i.e., $K = 2$ for the following numerical solution. The transition rate from *off* state to *on* state α_0 is chosen to be 1, while $\alpha_1 = 0.4$. When a source is in *on* state, it generates priority cells at rate $\lambda_0 = 1$ Mbits/s and marked cells at rate $\lambda_1 = 0.5$ Mbits/s. The channel capacity $c = 1.2$ Mbits/s, and the variance of the channel service rate is $\sigma^2 = 0.1$ Mbits/s. The buffer size X_m is chosen to be 10 Mbits, while the threshold value b is chosen to be 3 Mbits. The rate matrix R is therefore

$$R = \begin{cases} \text{diag}[-1.2, 0.3, 1.8], & 0 < x < b, \\ \text{diag}[-1.2, -0.2, 0.8], & b < x < X_m, \end{cases}$$

and the variance matrix Σ is

$$\Sigma = \begin{cases} \text{diag}[0.1, 0.1, 0.1], & 0 < x < b, \\ \text{diag}[0.1, 0.1, 0.1], & b < x < X_m. \end{cases}$$

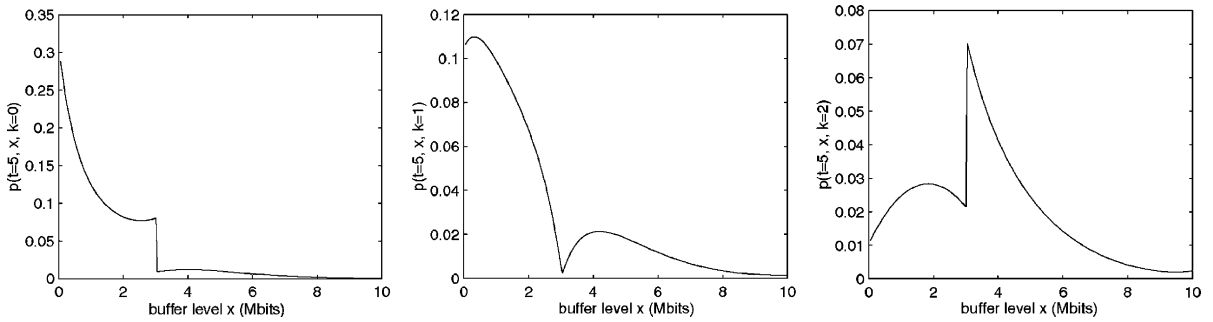


Fig. 2. Snapshot of $\mathbf{p}(t, x)$ at time $t = 5$ s.

At the boundary $x = 0$ (the lower boundary X_0), we have that $\sigma_0(0^+) = \sigma_1(0^+) = \sigma_2(0^+) = 0.1$. Therefore, at $x = 0$, states $k = 0, 1, 2$ are reflecting states. Similarly, at $x = X_m$ (the upper boundary), states $k = 0, 1, 2$ are also reflecting states.

At boundary $x = b$ (the intermediate boundary), $r_1(b^-) > 0$ and $r_1(b^+) < 0$, and hence state $k = 1$ is an absorbing state. Further note that $r_0(b^-) < 0, r_0(b^+) < 0$, and $r_2(b^-) > 0$ and $r_2(b^+) > 0$. Therefore, states $k = 0, 2$ are emitting states.

Above discussions lead to the following pmf $\mathbf{c}(t, x)$:

$$\mathbf{c}(t, x) = \begin{cases} [0, 0, 0], & X = 0, \\ [0, c(t, b, 1), 0], & X = b, \\ [0, 0, 0], & X = X_m. \end{cases}$$

Suppose that the initial buffer level is 0.2, and both of the traffic sources are in *off* state initially. Fig. 2 shows a snapshot of $\mathbf{p}(t, x)$ at $t = 5$ s. It is obvious from this figure that there is a jump in the probability density $p(t = 5, x, k = 1)$ and $p(t = 5, x, k = 3)$ at the location $x = 3$ Mbits. This result verifies the discussion on the boundary conditions that the probability mass accumulated under one environmental state will introduce abrupt changes of the probability density in other environmental states due to the transfer of probability mass.

By solving the equations for $\mathbf{c}(t, x)$ together with the equations for $\mathbf{p}(t, x)$, and integrating over x , we can get the CDF $\mathbf{P}(t, x)$. Fig. 3 shows a snapshot of $\mathbf{P}(t, x)$ at $t = 5$ s. Due to the probability mass accumulated

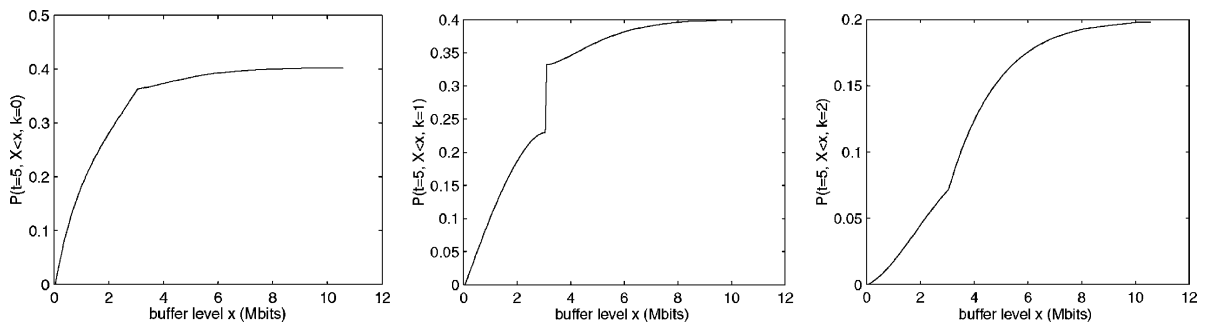


Fig. 3. Snapshot of $\mathbf{P}(t, x)$ at time $t = 5$ s.

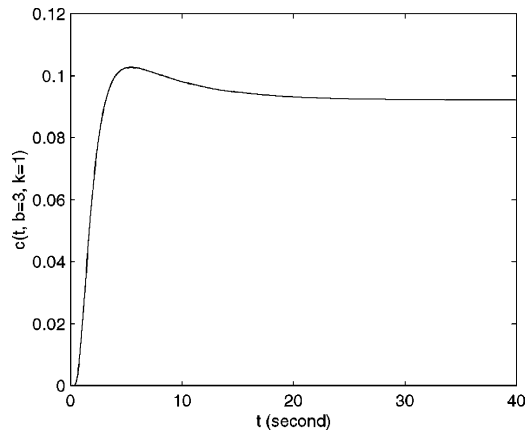


Fig. 4. Variation of $c(t, b = 3, 1)$ with time t .

at $x = 3$ Mbits under environmental state $k = 1$, there is an abrupt change in $P(5, x, 1)$ at $x = 3$ Mbits. For environmental states, $k = 0$ and 2 , no probability mass is accumulated and therefore there is no abrupt change for $P(5, x, 0)$ and $P(5, x, 2)$. However, since there is an abrupt change in their probability densities at $x = 3$ Mbits (refer to Fig. 2), the slopes of $P(5, x, 0)$ and $P(5, x, 2)$ change at this point.

Finally, Fig. 4 shows the transient behavior of the probability mass accumulated at boundary $x = 3$ under environmental state 1, which is $c(t, b = 3, k = 1)$. The “overshoot” behavior shown in this figure is important in determining the system performance during transient overload conditions [9].

6. Conclusion

In this paper, boundary conditions of second-order stochastic fluid models and corresponding transient analyses are discussed. First, the boundary conditions are proposed in several typical cases. Then an algorithm based on finite difference method for the transient study of fluid models with intermediate boundaries is given. Finally, the application of this class of models in the statistical multiplexing problems is shown with the results given numerically.

Acknowledgements

This research was supported in part by the Air Force Office of Scientific Research under MURI Grant No. F49620-00-1-0327, and in part by DARPA and US Army Research Office under Award No. C-DAAD19 01-1-0646. Any opinions, findings, and conclusions or recommendations expressed in this publication are those of the author(s) and does not necessarily reflect the view of the sponsoring agencies.

References

- [1] A.I. Elwalid, D. Mitra, Statistical multiplexing with loss priorities in rate-based congestion control of high-speed networks, *IEEE Trans. Commun.* 42 (11) (1994) 2989–3002.
- [2] V.G. Kulkarni, Fluid models for single buffer systems, *Frontiers Queueing: Models Appl. Sci. Eng.* (1997) 321–338.

- [3] Q. Ren, H. Kobayashi, Transient solutions for the buffer behavior in statistical multiplexing, *Perform. Eval.* 23 (1995) 65–87.
- [4] B. Sericola, Transient analysis of stochastic fluid models, *Perform. Eval.* 32 (1998) 245–263.
- [5] K. Wolter, Performance and dependability modelling with second-order fluid stochastic Petri nets, Ph.D. Thesis, Technical University of Berlin, Germany, 1999.
- [6] E.-J. Ang, J. Barria, The Markov modulated regulated Brownian motion: a second-order fluid flow model of a finite buffer, *Queueing Syst.* 35 (2000) 263–287.
- [7] R.L. Karandikar, V.G. Kulkarni, Second-order fluid flow models: reflected Brownian motion in a random environment, *Oper. Res.* 43 (1) (1995) 77–88.
- [8] C.-Y. Wang, D. Logothetis, K.S. Trivedi, I. Viniotis, Transient behavior of ATM networks under overloads, in: *Proceedings of the IEEE INFOCOM'96*, San Francisco, 1996.
- [9] D. Logothetis, K.S. Trivedi, The effect of detection and restoration times for error recovery in communication networks, *J. Network Syst. Manage.* 5 (2) (1997) 173–195.
- [10] J.M. Harrison, *Brownian Motion and Stochastic Flow Systems*, Wiley, New York, 1985.
- [11] S. Karlin, H. Taylor, *A Second Course in Stochastic Processes*, Academic Press, New York, 1975.
- [12] W. Feller, Diffusion processes in one dimension, *Trans. Am. Math. Soc.* (77) (1954) 1–31.
- [13] D. Chen, D.Y. Chen, Y. Cao, K.S. Trivedi, Boundary conditions in transient analysis of stochastic fluid flow models: a single buffer case with fluid-dependent rates, submitted for publication.



Dongyan Chen received his B.Eng. degree in electrical engineering from Southeast University, Nanjing, China, and his M.S. degree in communication engineering from Nanyang Technological University, Singapore, in 1995 and 1999, respectively. He is currently a Ph.D. candidate in Electrical and Computer Engineering Department, Duke University. His research interest is in discrete and fluid modeling techniques, and their applications to communication systems design and reliability/performance evaluations.



Yiguang Hong received his B.S. and M.S. from Department of Mechanics, Peking University, and his Ph.D. from Chinese Academy of Sciences in China. He is an Associate Professor in Institute of Systems Science, Chinese Academy of Sciences. He is a recipient of Guanzaozhi Award of Chinese Control Conference in 1997, Young Author Prize of the 14th IFAC World Congress in 1999, the US National Research Council Resident Research Associateship Award in 2000, and Young Scientist Prize of Chinese Academy of Science in 2001. He is also an IEEE Senior Member. His main research interests include non-linear dynamics, non-linear control, and reliability and performance analysis of computer and communication systems.



Kishor S. Trivedi holds the Hudson Chair in the Department of Electrical and Computer Engineering at Duke University, Durham, NC. He is the Duke-Site Director of an NSF Industry-University Cooperative Research Center between NC State University and Duke University for carrying out applied research in computing and communications. He has been on the Duke Faculty since 1975. He is the author of a well-known text entitled, *Probability and Statistics with Reliability, Queuing and Computer Science Applications*, published by Prentice-Hall; this text has been reprinted as an Indian edition; the second edition of this book has just appeared. He has recently published two other books entitled, *Performance and Reliability Analysis of Computer Systems*, published by Kluwer Academic Publishers and *Queueing Networks and Markov Chains*, John Wiley. His research interests are in reliability and performance assessment of

computer and communication systems. He has published over 300 articles and lectured extensively on these topics. He has supervised 35 Ph.D. dissertations. He is a fellow of the Institute of Electrical and Electronics Engineers. He is a Golden Core Member of IEEE Computer Society.

Kishor will be spending a sabbatical year beginning fall 2002 at IIT Kanpur where he will be Poonam and Prabhu Goel Professor in the Department of Computer Science and Engineering. He will also be a Fulbright Visiting Lecturer during that period.